JOURNAL OF VIROLOGY, Aug. 2009, p. 7547–7559 Vol. 83, No. 15
0022-538X/09/$08.00+0 doi:10.1128/JVI.00015-09

Restriction of Equine Infectious Anemia Virus by Equine APOBEC3 Cytidine Deaminases▽†

Jörg Zielonka,[1,3] Ignacio G. Bravo,[2] Daniela Marino,[1,3] Elea Conrad,[1] Mario Perković,[1,3] Marion Battenberg,[1] Klaus Cichutek,[1] and Carsten Münk[1,3]*

Division of Medical Biotechnology, Paul Ehrlich Institut, Langen, Germany[1]; Centre for Public Health Research, Valencia, Spain[2]; and Clinic of Gastroenterology, Hepatology and Infectiology, Heinrich Heine University, Düsseldorf, Germany[3]

Received 5 January 2009/Accepted 11 May 2009

The mammalian APOBEC3 (A3) proteins comprise a multigene family of cytidine deaminases that act as potent inhibitors of retroviruses and retrotransposons. The A3 locus on the chromosome 28 of the horse genome contains multiple A3 genes: two copies of A3Z1, five copies of A3Z2, and a single copy of A3Z3, indicating a complex evolution of multiple gene duplications. We have cloned and analyzed for expression the different equine A3 genes and examined as well the subcellular distribution of the corresponding proteins. Additionally, we have tested the functional antiretroviral activity of the equine and of several of the human and nonprimate A3 proteins against the *Equine infectious anemia virus* (EIAV), the *Simian immunodeficiency virus* (SIV), and the *Adeno-associated virus type 2* (AAV-2). Hematopoietic cells of horses express at least five different A3s: A3Z1b, A3Z2a-Z2b, A3Z2c-Z2d, A3Z2e, and A3Z3, whereas circulating macrophages, the natural target of EIAV, express only part of the A3 repertoire. The five A3Z2 tandem copies arose after three consecutive, recent duplication events in the horse lineage, after the split between Equidae and Carnivora. The duplicated genes show different antiviral activities against different viruses: equine A3Z3 and A3Z2c-Z2d are potent inhibitors of EIAV while equine A3Z1b, A3Z2a-Z2b, A3Z2e showed only weak anti-EIAV activity. Equine A3Z1b and A3Z3 restricted AAV and all equine A3s, except A3Z1b, inhibited SIV. We hypothesize that the horse A3 genes are undergoing a process of subfunctionalization in their respective viral specificities, which might provide the evolutionary advantage for keeping five copies of the original gene.

The *Equine infectious anemia virus* (EIAV) (family *Retroviridae*, genus *Lentivirus*) infects equids almost worldwide, causing a persistent infection characterized by recurring viremia, fever, thrombocytopenia, and wasting symptoms (40). EIAV infections are used as a model for natural immunologic control of lentivirus replication and virus persistence and as a test system to improve vaccines against lentiviruses (10, 40, 41, 82). In vivo EIAV replicates predominantly in macrophages (77). Interaction with the equine lentiviral receptor 1 (ELR1) has been demonstrated to be responsible for EIAV internalization (96). There have been no reported cases of EIAV infections in humans, suggesting that it is an intrinsically safe virus and of interest for use in a clinical setting. Therefore, EIAV-based lentiviral vectors for human gene therapy were recently developed (1, 67, 68).

In the last few years, two cellular proteins that inhibit many different retroviruses have been characterized: tripartite motif protein 5 alpha (TRIM5α) and apolipoprotein B mRNA-editing enzyme-catalytic polypeptide 3 (APOBEC3 [A3]) (for a review, see reference 92). With respect to TRIM5α proteins, both human and nonhuman primate TRIM5α orthologues can restrict infection by EIAV (26, 72). The activity of equine TRIM5α on EIAV infection, however, has not been described so far. With respect to A3 proteins, human APOBEC3G (A3G) is the best-characterized member of the A3 gene family. The ability of A3G to restrict EIAV was identified by Mangeat et al. during research focusing on the activity of the *Human immunodeficiency virus type 1* (HIV-1) viral infectivity factor (Vif) protein (48). The mechanism whereby A3G inhibits EIAV was not investigated. HIV-1 mutants lacking Vif package A3G into viral particles. Incorporated A3G specifically deaminates cytosine residues to uracil in growing single-stranded DNA during reverse transcription, leading to HIV genome degradation or hypermutation (5, 25, 39, 48, 49, 98). More recent studies indicate that deaminase-independent mechanisms might also be involved in antiviral activity of A3 (4, 27, 28, 30, 54, 61). The amount of encapsidated A3G in wild-type (wt) HIV-1 virions is dramatically reduced by a Vif-dependent degradation via the ubiquitination-proteasome pathway (50, 79, 94, 95). EIAV is the only extant lentivirus lacking a *vif* gene, a characteristic shared with *Rabbit endogenous lentivirus type K* (34). In contrast to the well-characterized A3-Vif interaction, still little is known about A3-neutralizing strategies used by retroviruses that do not encode a Vif protein. It has been reported that foamy retroviruses use the accessory protein Bet, and *Human T-cell leukemia virus type I* has evolved a unique nucleocapsid protein to counteract the packaging of cognate A3 proteins (12, 44, 58, 71). The debate over the mechanism of resistance to murine A3 (muA3) of the rodent gammaretrovirus *Moloney murine leukemia virus* (Mo-MLV) has not come up with a generally convincing model, despite many studies (5, 9, 13, 32, 35, 49). However, recent data

* Corresponding author. Mailing address: Clinic of Gastroenterology, Hepatology and Infectiology, Heinrich Heine University, Building 23.12.U1.87, Moorenstr. 5, 40225 Düsseldorf, Germany. Phone: 49 211 81 10887. Fax: 49 211 81 15431. E-mail: carsten.muenk@med.uni-duesseldorf.de.

† Supplemental material for this article may be found at http://jvi.asm.org/.

▽ Published ahead of print on 20 May 2009.

clearly show that muA3 is an important in vivo restriction factor of Mo-MLV and the Friend virus complex (45, 73, 89).

The evolution of the A3 genes appears as a complex, taxon-specific history of expansion, divergence, selection, and individual extinction of antiviral A3 that parallels in some points the early evolution of placental mammals (38, 58). Humans carry seven A3 genes, rodents carry one, pigs carry two, horses carry six, and cats carry four A3 genes (6, 31, 38, 58, 63). For the sake of clarity, the nomenclature for nonprimate A3s has been recently changed, based on the characteristics of the zinc (Z)-coordinating domain, to Z1, Z2, and Z3 (37). In light of the absence of a *vif* gene in EIAV and of a recent study of Bogerd et al. (6) on two equine A3s (eqA3s) (eqA3Z2a-Z2b and eqA3Z2c-Z2d, previously designated A3F1 and A3F2, respectively) that suggested that EIAV is resistant to eqA3s, we were interested in eqA3 genes and in the differential ability of the eqA3 proteins to restrict EIAV and other viruses.

Here, we identified and characterized five eqA3 proteins in regard to their activity against EIAV, *Simian immunodeficiency virus* (SIV), and *Adeno-associated virus type 2* (AAV-2). In contrast with a previous report (6), we identified eqA3s that strongly inhibited EIAV. The five eqA3s showed differential antiviral specificities against EIAV, SIV, and AAV, which we interpret as evidence for an ongoing subfunctionalization process. These results underpin the possibility that specific A3 paralogues protect against distinct viruses. The process of A3 gene duplication and subfunctionalization might result in an evolutionary advantage, enlarging the antiretroviral armory, and provide an explanation for the expansion of the A3 family in many mammalian species.

MATERIALS AND METHODS

Cells and transfections. The human cell lines 293T, 293, HeLa, and HOS (ATCC CRL-1543); the feline cell line CrFK (ATCC CCL-94); and equine macrophage-like cells EML-3C (20) were maintained in Dulbecco's high-glucose modified Eagle's medium (Biochrom, Berlin, Germany) supplemented with 10% fetal bovine serum, 2 mM L-glutamine, penicillin (100 units/ml), and streptomycin (100 μg/ml). Equine (*Equus caballus*) peripheral blood mononuclear cells (PBMCs) were isolated from heparin-treated whole blood by Histopaque-1077 (Sigma-Aldrich, Taufkirchen, Germany) gradient centrifugation and cultured after activation with phytohemagglutinin (3 μg/ml) for three days in RPMI 1640 medium (Biochrom, Berlin, Germany) containing 10% fetal bovine serum, 5×10^{-5} M 2-mercaptoethanol, 2 mM L-glutamine, and 100 units of human recombinant interleukin-2 per ml at 37°C and 5% CO_2. Monocyte-derived macrophages were purified from peripheral equine blood following a standard procedure (52). Briefly, monocyte-derived macrophages were purified from peripheral equine blood by gradient centrifugation through Histopaque. Cells were seeded in six-well plates in high-glucose Dulbecco's modified Eagle's medium with 15% horse serum (Biochrom, Berlin, Germany), 2 mM L-glutamine, penicillin (100 units/ml), and streptomycin (100 μg/ml). Nonadherent cells were removed after an overnight incubation, and any remaining adherent cells were incubated for 10 days. Plasmid transfections into 293T cells were performed with Lipofectamine LTX (Invitrogen, Karlsruhe, Germany) according the manufacturer's instructions.

Viruses and infections. EIAV single-cycle luciferase vectors (EIAV-luc) were produced by cotransfecting 293T cells with the following: pONY3.1 (55), pONY8.1luc, the vesicular stomatitis virus G protein (VSV-G) expression plasmid pMD.G (18), and an A3 expression plasmid or empty vector pcDNA3.1(+) (Invitrogen, Karlsruhe, Germany). Vector pONY8.1luc was derived from pONY8.1G (69), a self-inactivating vector variant of pONY8.0 (53) coding for enhanced green fluorescent protein and a deleted *env* region. The *egfp* gene in pONY8.1G was replaced by the firefly luciferase gene (luc3) using restriction sites SacII and NotI. The luciferase gene was amplified by PCR using $pSIV_{agm}$Luc (where agm indicates the African green monkey SIV host) (49) as a template and the primers Eluc.fw (5′-CCTCCGCGGCCCCAAGCTATGGAAGACGCCAAA-3′; SacII restriction site is underlined; where present, fw indicates forward and rv indicates reverse) and Eluc.rv (5′-AGGCGGCCGCTTTACACGGCGATCTTT-3′; NotI restriction site is underlined), subcloned in pJET1.2/blunt (Fermentas, St. Leon-Rot, Germany), sequence verified, and recloned into pONY8.1 using SacII and NotI restriction sites. The procedure used to generate pONY3.1Δ*DU* results in an in-frame deletion of 270 bp in the predicted dUTPase (DU) coding region (modified after Threadgill et al. [90]). By using pONY3.1 template DNA and the primer pair EIAV1.fw (5′-GCGCGCGGCGCCTGGCACCACCACAAGGGCCT-3′) and EIAV-dDU.rv (5′-TGAGTGCCCTGCATCTTCATCTCT-3′) and the pair EIAV2.rv (5′-GCGCGCGAATTCCCATTCCAGTCGTTCCTGG-3′) and EIAV-dDU.fw (5′-GCTGGGCACTCAAATTCCAGACAG-3′), the 5′ and 3′ fragments were amplified separately. The fragments were fused through overlapping extension PCR and cloned into pONY3.1 using restriction sites KasI and EcoRI. pONY3.1Δ*S2* was made as described in Mitrophanous et al. (55): the deletion from nucleotide 5345 to 5397 was made by PCR using overlapping primers EIAV-dS2.fw (5′-GTTATAAGGTTTGATATCAGCAT-3′) and EIAV-dS2.rv (5′-CATAGAATGCGATGCTGATATC-3′). SIV reporter virions were produced via transfection of 293T cells with $pSIV_{agm}$LucΔ*vif*, a VSV-G expression plasmid, and an expression plasmid for A3 or pcDNA3.1(+). Reverse transcriptase activity of viruses was quantified by using a Cavidi HS Lenti RT kit (Cavidi Tech, Uppsala, Sweden). For reporter virus infections, CrFK, EML-3C, or HOS cells were seeded at 2.0×10^3 cells/well 1 day before transduction in 96-well plates and then infected with reporter virus stocks normalized for reverse transcriptase. Firefly luciferase activity was measured 3 days post-transduction with a Steadylite HTS reporter gene assay system (PerkinElmer, Cologne, Germany), according to the manufacturer's directions, on a Berthold MicroLumat Plus luminometer. To generate recombinant AAV-2, 293 cells were transfected with the *lacZ* reporter plasmid pAAV-lacZ (51, 93), the *rep-cap* encoding plasmid pAAV-RC (51, 93), the adenovirus helper plasmid pHelper (51, 93), and an expression plasmid for A3 or pcDNA3.1(+). Cells were harvested for analysis after 72 h. Lysate containing virions was generated by freeze/thaw cycles, and supernatants were used to transduce fresh 293 cells. Transduction was quantified 3 days later by measuring β-galactosidase activity using a GalactoStar kit (Applied Biosystems, Darmstadt, Germany) according to the manufacturer's instructions.

A3 expression and plasmids. All A3s are expressed as carboxy-terminal (CT) hemagglutinin (HA)-tagged proteins, except human A3DE (also known as human A3Z2c-Z2d), a gift from Y.-H. Zheng, that carries a CT V5 tag (11). The human A3G and muA3 expression constructs (human A3Z2g-Z1c and muA3Z2-Z3) were provided by N. R. Landau (49). Human A3B, -C, -F, and -H (A3Z2A-Z1b, A3Z2b, A3Z2e-Z2f, and A3Z3); feline A3; and canine A3 expression plasmids were previously described (33, 44, 57, 58). Porcine A3 (A3Z2-Z3) was a gift of Eva Dörrschuck and Ralf Tönjes (GenBank accession no.EU871587; E. Dörrschuck et al., unpublished data). eqA3 cDNAs were identified by using 5′ and 3′ rapid amplification of cDNA ends reactions (5′/3′-RACE kit; Roche Diagnostics, Mannheim, Germany) employing total RNA from equine PBMCs. For expression plasmids of eqAPOBEC3Z1b (eqA3Z1b), the primers were E-APO-37 (5′-TTCGTGAATTCGGGACTGAGACATGGAGGCC-3′; forward) and E-APO-38 (5′-AGAGCTCGAGTCAAGCGTAATCTGGAACATCGTATGGATACCCAGAGGAGCCTCTGAGTG-3′; reverse); for eqA3Z2e, the primers were E-APO-27 (5′-ACGTGGTACCTACGTCCAGGCTCCCAGGAAC-3′; forward) and E-APO-28 (5′-TTCTCTCGAGTCAAGCGTAATCTGGAACATCGTATGGATACTTGAGAATGTCCTCAAGCTTTG-3′; reverse); for eqA3Z2a-Z2b and eqA3Z2c-Z2d, the primers were primer E-APO3Ca/c-KpnI.fw (5′-ACGTGGTACCACCCAATGGAGAAGTTGGAT-3′; where present, fw indicates forward and rv indicates reverse) and E-APO3Cb-XhoI.rv (5′-GCGCCTCGAGTCAAGCGTAATCTGGAACATCGTATGGATACTTGAGAAGGTCCT-3′) or E-APO3Cd-XhoI.rv (5′-GCGCCTCGAGTCAAGCGTAATCTGGAACATCGTATGGATACTTGAGAATCTCCT-3′); for eqA3Z3, the primers were E-APO-35 (5′-TTCGTGAATTCGAGGTCACTCTCAGATAAGCGGC-3′; forward) and E-APO-36 (5′-AGAGCTCGAGTCAAGCGTAATCTGGAACATCGTATGGATACCCGAGGTCAACCGACCCAAG-3′; reverse); *Pwo* polymerase (Roche Applied Science, Mannheim, Germany) was used. Each of 30 cycles was run at 94°C for 30 s, 58°C for 1 min, and 72°C for 2 min. PCR products were cloned into pcDNA3.1(+) using restriction sites KpnI or EcoRI and XhoI, and sequences were verified. EA3F2 (6) was made by exchanging amino acids (V40G, P48V, S339I, and K354N) of the eqA3Z2c-Z2d template through overlapping extension PCR, and the resulting cloned PCR product was sequence verified. eqA3Z3 point mutants were generated by exchanging zinc-coordinating amino acids (H84R, C115S, and C118S) or the catalytic glutamic acid residue (E86Q) through overlapping extension PCR. The 5′ and 3′ fragments were amplified separately by using primer E-APO-35 containing an EcoRI site or the 3′ primer E-APO-36 containing an XhoI site. The 5′ and 3′ fragments were then mixed and amplified with the two external primers. The resulting full-length mutant was cleaved with restriction enzymes and cloned into pcDNA3.1(+) and sequence verified. The human A3F and A3G point mutants have been described previously (7,

23). A3F mutants h3FAS1 (E67A), h3FAS2 (E251A), and h3FAS1/AS2 (E67A/E251A) were a gift of N. R. Landau; the mutant A3G-E259Q was a gift of Barbara Schnierle. Expression studies of eqA3 RNA of PBMCs, macrophages, and spleen cells were done by reverse transcription-PCR (RT-PCR) using total RNA, *Taq* polymerase (Fermentas, St. Leon-Rot, Germany), and the primers E-APO-3 (5′-AGACACCTTCACTGAGAACTTC-3′; forward) and E-APO-2 (5′-ATGGACCAGTAGCGACTCTCA-3′; reverse) for eqA3Z1a and eqA3Z1b; the primers rtE-A3Ce.fw (5′-TTGCATCCCAAGACCTCC-3′; where present, fw indicates forward and rv indicates reverse) and rtE-A3Ce.rv (5′-GGTACTGCTTCATGAAGTCA-3′) for eqA3Z2e; the primers rtE-A3Ca.fw (5′-GTGATGTTGCGCAAGGA-3′) and rtE-A3Cb.rv (5′-CCCTTGGCAAATTTCAG-3′) for eqA3Z2a-Z2b; the primers rtE-A3Cc.fw (5′-TGACACTGGCGGCCA-3′) and rtE-A3Cd.rv (5′-TCCGGCTTATTCCTTTGC-3′ for eqA3Z2c-Z2d; and the primers E-APO-23 (5′-CAGACCCACAATGAATCCAC-3′; forward) and E-APO-26 (5′-CTGCTGATTCTGCCTGAACCAG-3′; reverse) for eqA3Z3. The housekeeping gene for human glyceraldehyde 3-phosphate dehydrogenase (GAPDH) served as an internal control for RT-PCR using forward primer human GAPDH A (5′-GTTGCCATCAATGACCCCTTCATTG-3′) and reverse primer human GAPDH B (5′-GCTTCACCACCTTCTTGATGTCATC-3′). To detect ELR1, RT-PCR and primer ELR1.fw (5′-CCAAGGCTGATGCCCTGAGC-3′) and primer ELR1.rv (5′-GGCCTGGCAGCTCTCGGCAG-3′) were used to verify equine cDNA. PCRs were run for 30 cycles of 94°C for 30 s, 1 min at 60°C, and 72°C for 2 min.

Quantitative real-time PCR analyses of eqA3 mRNA. Total RNA was isolated from equine PBMCs and macrophages using an RNeasy minikit (Qiagen, Hilden, Germany), according to the manufacturer's instructions. Isolated RNA was reverse transcribed with QuantiTect Reverse Transcription (Qiagen, Hilden, Germany). The eqA3 fragments were amplified from cDNA and quantified using SYBR green PCR Master Mix (Applied Biosystems, Warrington, United Kingdom) with an Applied Biosystems 7500 Real-Time PCR system (Applied Biosystems, Foster City, CA) and A3-specific primers as follows (fw indicates forward and rv indicates reverse): qPCR-A3Ccd.fw (5′-ACCATCATGGAAGGCACTTCATTCC-3′) and qPCR-A3Ccd.rv (5′-TGCAGCTTCTCCAATGGGTTTTTGA-3′) for A3Z2c-Z2d; qPCReq3Ce.fw (5′-AGTGGAAGGAAGGTTGAGCGGC-3′) and qPCReq3Ce.rv (5′-CGGAACCAATCGAGGAAGCAGA-3′) for A3Z2e; and qPCReq3H-2.fw (5′-CCGGGAACGGAAACACACAGCATC-3′) and qPCReq3H-2.rv (5′-ACGGAGCAGCTTCAGCTGGTAGCA-3′) for A3Z3. After initial incubations at 50°C for 2 min and 95°C for 10 min, 40 cycles of amplification were carried out for 15 s at 95°C, followed by 1 min at 60°C. The amplification product was normalized to that of equine GAPDH.

Sequencing of viral transcripts. CrFK cells (1×10^6) were infected with DNase I (Roche, Mannheim, Germany)-treated EIAV-luc (VSV-G pseudotyped) (1,000 pg of reverse transcriptase) using pONY8.1luc, pONY3.1, and pMD-G produced in 293T cells together with eqA3s or pcDNA3.1(+). At 10 h postinfection, cells were washed with phosphate-buffered saline (PBS), and DNA was isolated using a DNeasy DNA isolation kit (Qiagen, Hilden, Germany). An 880-bp fragment of the luciferase gene was amplified using *Taq* DNA polymerase (Fermentas, St. Leon-Rot, Germany) and the primers 5′luc3@812nt (5′-GATATGTGGATTTCGAGTCGTC-3′) and Eluc.rv (5′-AGGCGGCCGCTTTACACGGCGATCTTT-3′). Each of 30 cycles was run at 95°C for 30 s, 50°C for 1 min, and 72°C for 2 min. For better selective amplification of hypermutated viral genomes, the PCR denaturation temperature was lowered to 88°C (30 cycles of 1 min at 88°C, 1 min at 50°C, and 2 min at 72°C). The PCR products were cloned into pJet1.2/blunt vector (Fermentas, St. Leon-Rot, Germany) and sequenced. The nucleotide sequences of at least 10 independent clones were analyzed.

Immunoblot analysis. Cells were cotransfected with plasmids for viral vectors of EIAV and A3 expression plasmids, and lysates were prepared 2 days later. Cell lysates were prepared by removing the medium from transfected cells, washing them with PBS, and lysing them in radioimmunoprecipitation assay buffer (25 mM Tris · HCl, pH 7.6, 150 mM NaCl, 1% NP-40, 1% sodium deoxycholate, 0.1% sodium dodecyl sulfate). Virions were pelleted by centrifugation of filtered (0.45-μm-pore size) culture supernatant through a 20% sucrose cushion at 35,000 rpm in an SW40Ti rotor for 1.5 h and resuspended with radioimmunoprecipitation assay buffer. Protein concentration in the lysates was quantitated using Bradford reagent (Bio-Rad, Munich, Germany). Lysates containing 20 μg of protein were separated by sodium dodecyl sulfate-polyacrylamide gel electrophoresis and transferred to polyvinylidene difluoride filters. Filters were probed with mouse anti-HA antibody (1:10,000 dilution; MMS-101P; Covance, Münster, Germany), mouse anti-V5 antibody (1:5,000 dilution; MCA1360; ABDserotec, Düsseldorf, Germany), or a mixture of both or with mouse anti-α-tubulin antibody (1:4,000 dilution; clone B5-1-2; Sigma-Aldrich, Taufkirchen, Germany) or mouse anti-VSV-G antibody (1:10,000 dilution; clone P5D4, Sigma-Aldrich, Taufkirchen, Germany), followed by horseradish peroxidase-conjugated rabbit anti-mouse antibody (α-mouse immunoglobulin G-horseradish peroxidase; GE Healthcare, Munich, Germany), and developed with ECL chemiluminescence reagents (GE Healthcare, Munich, Germany).

Immunofluorescence. HeLa cells grown on polystyrene coverslips (Thermo Fisher Scientific, Langenselbold, Germany) were transfected with A3 expression plasmids by applying FuGENE (Roche Applied Science, Mannheim, Germany) transfection reagent (DNA-FuGENE ratio of 1:3). At 1 day posttransfection, cells were fixed in 4% paraformaldehyde in PBS for 30 min, permeabilized in 0.1% Triton X-100 in PBS for 45 min, incubated in blocking solution (10% donkey antiserum [Sigma-Aldrich, Taufkirchen, Germany] in PBS) for 1 h, and treated with anti-HA antibody (MMS-101P; Covance, Münster, Germany) and anti-nucleolin (ab22758; Abcam, Cambridge, United Kingdom) in a 1:1,000 dilution in blocking solution for 1 h. Donkey anti-mouse Alexa Fluor 488 (Invitrogen, Karlsruhe, Germany) and anti-rabbit Alexa Fluor 594 were used as secondary antibodies in a 1:300 dilution in blocking solution for 1 h. Finally, nuclei were stained using DAPI (4′,6′-diamidino-2-phenylindole; 1:1000 in PBS) (Millipore, Billerica) for 5 min. The images were captured by using a 40× objective on a Zeiss LSM 510 Meta laser scanning confocal microscope. Optical sections were acquired from 1-μm-thick layers.

Phylogenetic analysis. All A3 sequences in the databases from mammalian species within Laurasiatheria were retrieved for analysis, as follows: *Sus scrofa*, A3Z2 (NM_001097446); *Bos taurus*, A3Z1 (EU864534), A3Z2 (NM_001077845), and A3Z3 (DQ974646); *Ovis aries*, A3Z1 (EU864543), A3Z2 (EU864535), and A3Z3 (NM_001093784); *Canis lupus*, A3Z3 (XM_538369) and A3Z1 (XM_847690); *Felis catus*, A3Z3 (NM_001112710), A3Z2a (ABW83272), A3Z2b (ABW83273), and A3Z2c (ABW83271); *Lynx lynx*, A3Z3 (EU007553) and A3Z2 isolate 1 (EU007546); *Puma concolor*, A3Z2 (EU007545); *Panthera pardus*, A3Z3 (EU007551) and A3Z2 (ABA62303); *Panthera leo*, A3Z3 (U007549), A3Z2 isolate 7 (EU007543), and A3Z2 isolate 2 (EU007544); *Panthera tigris*, A3Z3 (EU007550), A3Z2 (AAY99623), A3Z2 isolate 2 (EU016361), and A3Z2 isolate 3 (EU016362). The sequences were aligned at the amino acid level with MUSCLE (http://www.drive5.com/muscle/) (15, 16), visualized for manual correction with Se-Al (freely distributed by Andrew Rambaut at http://tree.bio.ed.ac.uk/software/seal/), and back-translated to the nucleotide level using PAL2NAL (http://www.bork.embl.de/pal2nal) (88). Maximum-likelihood (ML) phylogenetic analysis was performed with the program RAxML HPC (randomized accelerated maximum likelihood for high performance computing) (84, 85) using the GTR+Γ4 model of evolution and the CAT approximation of rate heterogeneity (83), introducing three partitions that corresponded to each of the codon positions. Four independent runs of 1,000 bootstraps were performed, and for each the final tree topology was optimized without resorting to the CAT approximation. The best of the four final trees was chosen ($-\ln = 8697.653751$; respective optimized values for the alpha parameter of the gamma function for each codon position were 1.312, 1.015, and 4.327), but there were no significant differences among the corresponding likelihood values using an SH (for Shimodaira and Hasegawa) test (80). Bootstrap support values for the nodes were obtained from the combined four sets of 1,000 trees. A pairwise distance matrix was also generated under the ML framework. Bayesian phylogenetic analysis was performed with BEAST, version 1.4.7 (http://beast.bio.ed.ac.uk) (14), with the GTR+Γ4 model of evolution and for both strict clock and uncorrelated log normal relaxed clock, introducing three partitions that corresponded to each of the codon positions, and unlinking parameters across codon positions. Two independent chains of 50 million steps were calculated, writing every 1,000 steps, and analyzed with a burn-in of 10 million steps. Compatibility of both chains was assessed by calculating the corresponding Bayes factor (86), and both chains were combined into one. The combined chains from the relaxed and the strict clock were also compared by calculating the Bayes factor on the corresponding likelihoods. There was only marginally better support for the relaxed clock calculations (log Bayes factor, 2.1). The Bayesian maximum clade credibility tree was built based on the relaxed clock combined chain, and its likelihood was calculated under ML framework and compared with the best RAxML tree. The Bayesian tree was worse than the best ML tree, albeit not significantly worse in an SH test ($-\ln = 8713.565178$; score difference between the log ML values for the trees, −15.911427; standard deviation of the score difference after nonparametric bootstrap, 11.028095) (80). The Bayesian posterior probabilities were therefore calculated by projecting the trees from the combined Bayesian chain onto the best ML tree. The reference cladogram for the animal species included in the taxon sample was pruned out from a mammalian tree constructed after the supertree methodology (3), using TREEPRUNER (freely distributed by Olaf Bininda-Emonds at http://www.uni-oldenburg.de/molekularesystematik/33997.html).

Nucleotide sequence accession numbers. The sequences reported here have been deposited in the GenBank database (accession number): eqA3Z1b

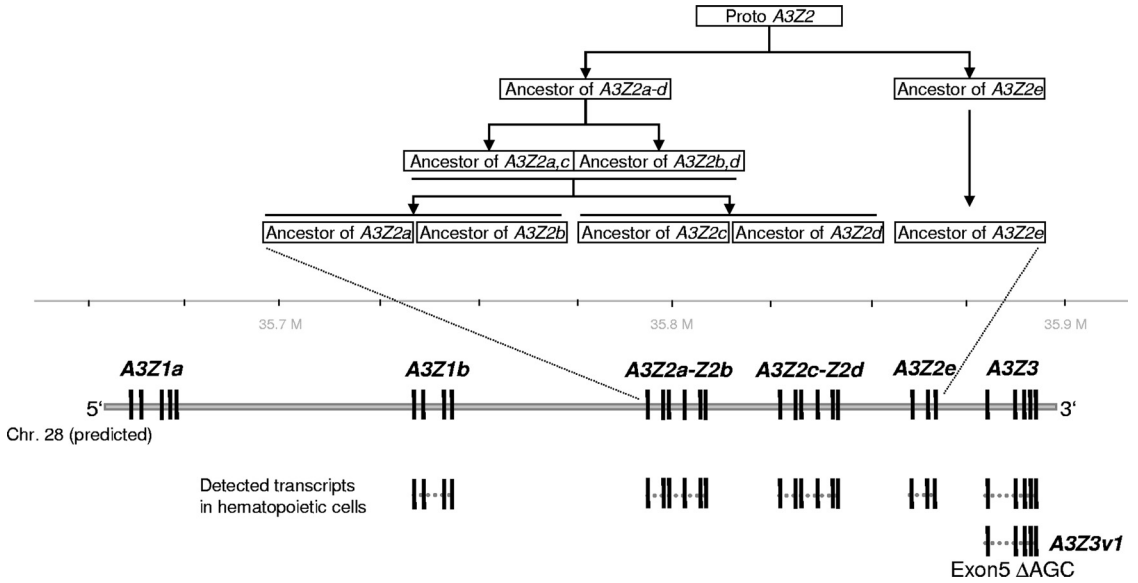

FIG. 1. Identification of A3 coding regions in the genome of *Equus caballus*. Representation of the eqA3 genomic region showing the exon/intron organization of the A3 genes. Transcripts with exons (rectangles) and spliced-out introns (dotted lines) are indicated. Please note that the two eqA3Z3 cDNAs differ in a lack of three nucleotides (AGC) at the 3′ end of the A3Z3v1 coding region. The recent study of Bogerd et al. used a different nomenclature for the eqA3 genes: A3A1 for A3Z1a, A3A2 for A3Z1b, A3F1 for A3Z2a-Z2b, A3F2 for A3Z2c-Z2d, A3C for A3Z2e, and A3H for A3Z3 (6). Chr, chromosome.

(FJ532287), eqA3Z2a-Z2b (FJ527822), eqA3Z2c-Z2d (FJ527823), eqA3Z2e (FJ532288), eqA3Z3 (FJ532289), and eqA3Z3v1 (FJ532286).

RESULTS

The evolution of eqA3 implies several gene duplications. In the genome sequence from the horse whole-genome assembly, released by the Broad Institute of MIT/Harvard (NCBI GenBank accession no. NW_001799702), we identified six predicted A3 genes: A3Z1a, -Z1b, -Z2a-Z2b, -Z2c-Z2d, -Z2e, and -Z3. The different A3 genes in the horse genome span ca. 0.25 Mb of the chromosome 28, and closely related genes are clearly organized in tandem repeats (Fig. 1). The phylogenetic relationships of the A3 genes within the placentalia superorder of Laurasiatheria are depicted in Fig. S1 in the supplemental material. Phylogenies reconstructed with ML and with Bayesian methodologies were mainly congruent, with the exception of some ill-defined nodes. Thus, three main clusters can be observed, corresponding to the A3Z1, -Z2, and -Z3 proteins. Each of these clusters reflects grossly the topology of the corresponding species and encompasses genes from different mammalian orders within Laurasiatheria (see Fig. S1 in the supplemental material). Finally, the phylogenetic relationships among eqA3Z2s suggest that the five copies forming the present three genes have appeared after three recent duplication events (Fig. 1).

Identification of A3 RNAs in equine cells. To functionally characterize eqA3s, total RNAs from activated equine PBMCs and equine spleen cells were tested by a combination of RT-PCR and techniques used in 5′/3′ rapid amplification of cDNA ends (Fig. 2A). From these sources, we cloned six equine cDNAs (eqA3Z1b, -Z2a-Z2b, -Z2c-Z2d, -Z2e, -Z3, and -Z3v1). The two eqA3Z3 cDNAs differ in a lack of 3 nucleotides (AGC) at the 3′ end of the A3Z3 coding region. RNA of the predicted gene for eqA3Z1a could not be identified in hematopoietic cells (Fig. 2A). It has been shown that the in vivo tropism of EIAV is restricted to cells of the monocyte-macrophage lineage (76, 77). Therefore, equine macrophage-derived RNA was examined by RT-PCR using eqA3-specific primers. Using semiquantitative PCR on macrophage total RNA, we could detect A3Z2a-Z2b, -Z2c-Z2d, and -Z2e transcripts while we failed to amplify any A3Z1 and -Z3 transcripts (Fig. 2A). Quantitative real-time PCR showed that macrophages express ~19-fold lower levels of A3Z3 than PBMCs (Fig. 2B).

The nomenclature classification of the eqA3s is based on their phylogenetic relationships (see Fig. S1 in the supplemental material) and zinc (Z)-coordinating domain assignments (37): eqA3Z1b has a 45.4% amino acid identity to human A3A(A3Z1a); eqA3Z2a-Z2b and eqA3Z2c-Z2d have 42.9% and 44.3% amino acid identity to human A3F (A3Z2e-Z2f), respectively; eqA3Z2e a has 45% amino acid identity to human A3C (A3Z2b); and eqA3Z3 shares 40.4% identical amino acids with human A3H (A3Z3) (see Fig. S2 in the supplemental material). We used the cloned eqA3Z1b, -Z2a-Z2b, -Z2c-Z2d, -Z2e, -Z3, and -Z3v1 cDNAs to generate expression plasmids for HA-tagged A3s. To characterize subcellular distribution of A3s, cells expressing eqA3s were analyzed by using an anti-HA antibody in confocal microscopy (Fig. 2C). Immunofluorescence studies of transiently expressed eqA3Z1b in HeLa cells showed a strict nuclear localization, as previously reported also for human A3A (57). The subcellular distribution of eqA3Z2a-Z2b is limited to the cytoplasm, and eqA3Z2c-Z2d is localized in the nucleus. In contrast to human A3C that displays a cytoplasmic and nuclear distribution (57), the eqA3Z2e could be detected only in the cytoplasm. The eqA3Z3 and eqA3Z3v1 and the human A3H are distributed in the cytoplasm and in

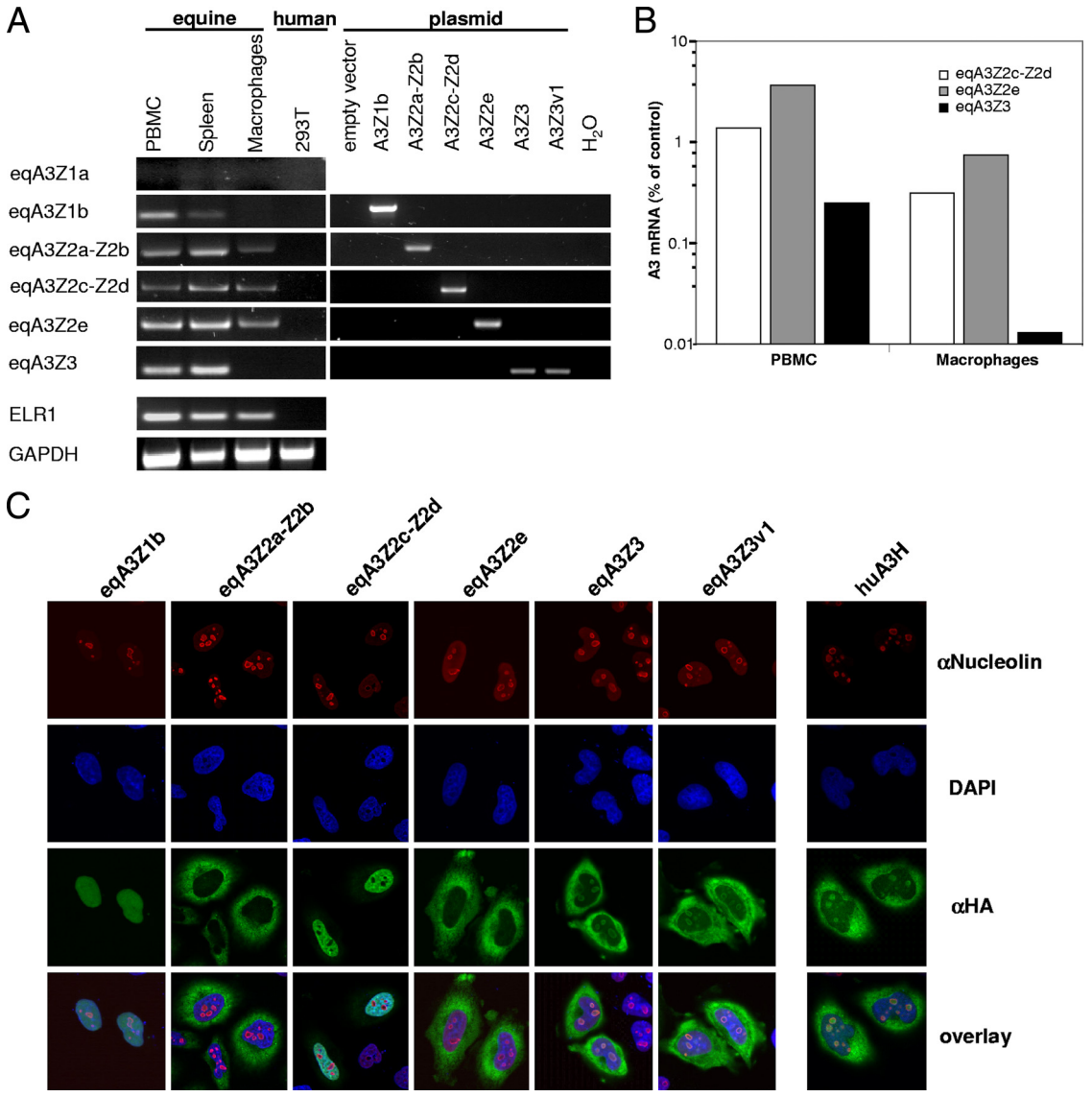

FIG. 2. Differential expression of eqA3s. (A) Analysis of eqA3Z1a, eqA3Z1b, eqA3Z2a-Z2b, eqA3Z2c-Z2d, eqA3Z2e, and eqA3Z3 expression by RT-PCR of total RNA from equine activated PBMCs, spleen cells, and macrophages. Primer specificity in PCR was tested by using eqA3 plasmids as templates. PCRs were performed with specific primers to amplify ELR1 for species control, and GAPDH served as a loading control. (B) eqA3Z3 is expressed at a significantly lower level in macrophages. RNA was extracted from both equine PBMCs and macrophages. Levels of A3 expression were determined by quantitative real-time RT-PCR and expressed relative to the levels of the GAPDH RNA. (C) eqA3s show a different subcellular localization. HeLa cells were transfected with HA-tagged eqA3Z1b, eqA3Z2a-Z2b, eqA3Z2c-Z2d, eqA3Z2e, and eqA3Z3 and with human A3H and A3Z3. To detect A3 (green) immunofluorescence, staining was performed with an anti-HA antibody. Nuclei (blue) were visualized by DAPI staining. Nucleolar nucleolin protein (red) was detected with anti-nucleolin antibody. α, anti; hu, human.

nuclear bodies (Fig. 2C). Costaining with an antibody against the nucleolar nucleolin protein revealed that eqA3Z3 and human A3H localize in the nucleolus to the nucleoli.

eqA3 proteins restrict EIAV, SIV_{agm}, and AAV-2. To examine the restriction activity of eqA3 proteins, VSV-G pseudotyped EIAV-luc and SIV_{agm}-luc reporter viruses were generated in human 293T cells in the presence of cotransfected eqA3 expression plasmids. Reverse transcriptase-normalized EIAV vector particles were used to transduce feline CrFK cells because they show no Trim5α-dependent postentry restriction of EIAV (72, 97). Infectivity of SIV vectors was analyzed by infection of human HOS cells. At 3 days postinfection the cells were lysed and used to quantify intracellular luciferase activity. In addition, we tested the inhibitory capacity of the eqA3s on the transduction of AAV-2-lacZ reporter vectors. We found that the eqA3 expression plasmids produced functional active antiviral proteins and that most showed a distinct specificity against different viruses (Fig. 3A to C). All six eqA3 proteins were detectable in purified EIAV particles by immunoblotting (Fig. 3D), suggesting that no viral factor induced their exclusion from EIAV virions. eqA3Z3 restricted any tested viruses: EIAV infectivity was reduced by a factor 60, SIV was reduced by factor 13, and AAV-2 was fivefold inhibited (Fig. 3A to C). The eqA3Z1b and -Z2e showed only moderate activity on

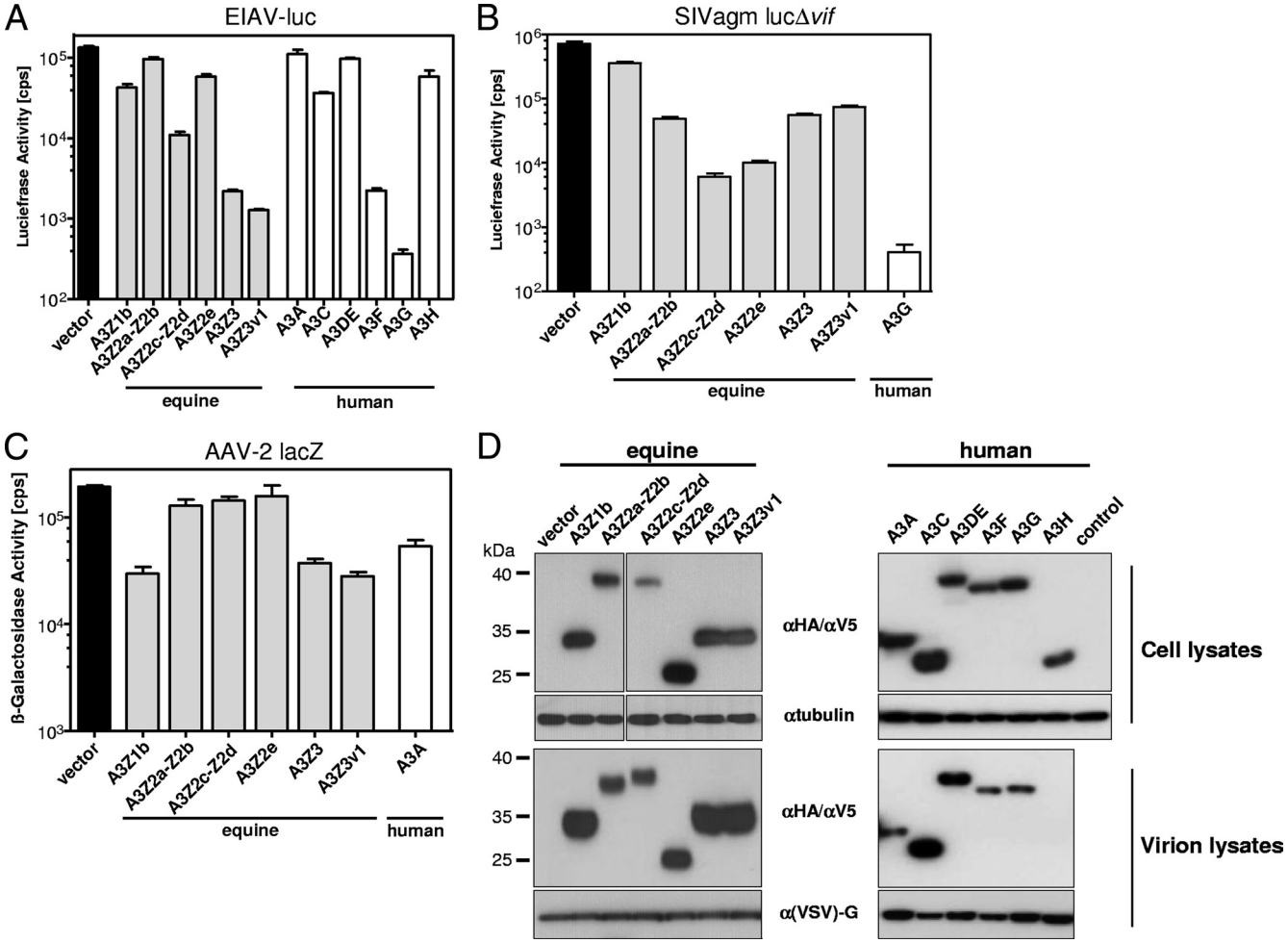

FIG. 3. eqA3 proteins inhibit the infectivity of different viruses. (A) EIAV-luc (VSV-G pseudotyped) was produced in 293T cells in the presence or absence of the indicated equine and human A3s. Infectivity of the viruses was determined by quantification of luciferase activity in CrFK cells with equal amounts of viruses at 3 days postinfection. (B) SIV_{agm} Δ*vif* viruses were produced in the presence or absence of the indicated A3 proteins. Infectivity of normalized amounts of viruses was determined by quantification of luciferase activity at 3 days postinfection. (C) AVV-2 viruses were generated by transfecting 293 cells in the presence or absence of the indicated A3 proteins. Antiviral activity of A3 proteins was determined by quantification of ß-galactosidase expression at 3 days postinfection. (D) Equine and human A3 proteins are packaged in EIAV virions. Virions were generated by cotransfection of 293T cells with EIAV-luc and HA- or V5-tagged equine and human A3 expression plasmids or pcDNA3.1 (vector). A3 expression in transfected cells was detected by immunoblotting using a mixture of anti-HA and anti-V5 antibodies. Cell lysates were also analyzed for equal amounts of total proteins by using anti-tubulin antibody. Packaged A3s in virions (normalized by RT activity) were detected by probing with anti-HA and anti-V5 antibody together on a parallel immunoblot. Immunoblots of virions were also probed with anti-VSV-G antibody as a control for the equal amounts of analyzed virions. cps, counts per second; α, anti.

EIAV and reduced the infectivity by approximately threefold each (Fig. 3A). Similarly, eqA3Z1b was weakly active against SIV. In contrast, SIV_{agm} infectivity was inhibited 70-fold by eqA3Z2e, and eqA3Z1b reduced the infectivity of AAV-2 by 10-fold (Fig. 3B and C). eqA3Z2c-Z2d restricted both EIAV and SIV by a factor of 12 and a factor of 120, respectively (Fig. 3A and B). Our results on the activity of A3Z2c-Z2d are in contrast to the report of Bogerd et al. (6). Comparing the sequence of A3Z2c-Z2d of Bogerd et al. (6), designated A3F2, with our A3Z2c-Z2d expression plasmid revealed four different amino acids (V40G, P48V, S339I, and K354N) (see Fig. S3 in the supplemental material). We introduced these amino acid changes in our construct and tested A3F2 for its antiviral activity (Fig. 4A). Both A3 proteins showed similar protein expression levels (Fig. 4B) and identical subcellular distributions (Fig. 2C) (compare to reference 6), but A3F2 reduced the infectivity of EIAV only twofold (Fig. 4A), confirming the results of Bogerd et al. (6). We conclude that natural sequence variants of some eqA3s can have a strong impact on their activity against EIAV.

To address the question whether eqA3 proteins show a cytidine deaminase activity, EIAV vector cDNAs were analyzed by PCR. We recovered an ~880-bp fragment of the luciferase gene from infected cells, 10 h postinfection. The rate of the detected G→A mutations in viral RT products was very low. The G→A mutation rate was equal to or less than 0.07% of all nucleotides for eqA3Z2a-Z2b, -Z2c-Z2d, and -Z3, and no G→A mutations were detectable for eqA3Z1a and -Z2e (Fig. 5A, left panel). Based on the unsatisfactory results for deamination activity of eqA3 proteins, we modulated the PCR con-

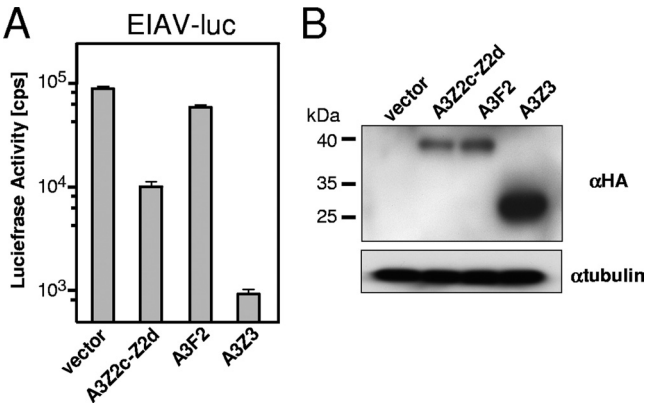

FIG. 4. Double domain eqA3Z2c-Z2d protein variants differ in their antiviral activity. (A) Single-cycle infectivity assays were performed for EIAV in presence or absence of A3Z2c-Z2d and the variant A3F2 differing in four amino acids. Infectivity of equal amount of viruses was determined by quantification of luciferase activity. (B) Immunoblot analysis of the indicated eqA3 proteins using an HA tag-specific antibody. α, anti; cps, counts per second.

ditions to selectively amplify AT-rich DNA generated by G→A hypermutations, as previously described for a three-dimensional PCR method (87). Indeed, the rate of G→A mutations detected by PCR using a denaturation temperature of 88°C was ~7% of all nucleotides for eqA3Z3 and ~3% for A3Z2c-Z2d (Fig. 5A, right panel; see also Table S1 in the supplemental material). In experiments with eqA3Z1b, -Z2a-Z2b, and -Z2e, a low rate of 0.2 to 0.5% G→A mutations was now detected, corresponding to their very weak antiviral activity against EIAV. Under this PCR condition, no amplification product was detectable in experiments omitting eqA3. The editing context of the G→A exchanges in EIAV genomes displays a dinucleotide preference of GG→AG and GA→AA (Fig. 5B). In conclusion, eqA3s harbor the intrinsic activity to deaminate cytidines and can deaminate EIAV genomes in at least a subpopulation of the transducing particles under experimental conditions.

The dUTPase and S2 genes do not affect the susceptibility of EIAV to eqA3s. EIAV encodes two genes, dUTPase (DU) and S2, that are absent in the genome of HIV-1. To investigate the possibility that DU or S2 counteracts the antiviral activity of eqA3s, EIAV DU and S2 mutation constructs were generated. Since there were no antibodies against DU and S2 available, no further biochemical studies on these proteins were performed. Two EIAV-packaging constructs were tested in which either the *DU* gene was inactivated by an in-frame deletion of 270 bp (EIAVΔ*DU*) identical to the method of Threadgill et al. (90) or the *S2* gene was inactivated by a deletion of 52 bp including the ATG start codon of S2 (EIAVΔS2), as described previously (55). We produced EIAV vectors of wt, ΔDU, or ΔS2 with and without expression plasmids for eqA3s and measured the particle infectivity on feline CrFK cells and on the equine macrophage-like cell line EML-3C. The results shown in Fig. 6 demonstrate that deletion of DU or S2 did not change the antiviral activities of the eqA3Z2a-Z2b or -Z2e that are inactive against wt EIAV. Moreover, wt, ΔDU, and ΔS2 vectors were equally inhibited by eqA3Z1b, -Z2c-Z2d, and -Z3. Thus, we conclude that the resistance of EIAV to eqA3Z2a-Z2b and -Z2e is not based on the function of the dUTPase or the S2 protein and that DU and S2 are not required for transduction of equine macrophage-like cells.

EIAV restriction by human and nonprimate A3 proteins. Previous studies investigated exclusively whether human A3A and human A3G are antiviral active against EIAV (6, 48). To determine if other human and nonprimate A3 proteins exert an inhibitory effect on the infectivity of EIAV, we cotransfected 293T cells with the EIAV-luc reporter vector together with expression plasmids encoding human A3A, -B, -C, -DE, -F, -G, or -H; feline A3Z2a, -Z2b, -Z2c, -Z3, or Z2b-Z3; canine A3Z1, or -Z3; porcine A3Z2-Z3; or muA3Z2-Z3. In experiments using the human A3B expression plasmid, no RT activity after cotransfection with the EIAV vector system was detectable in the cell supernatant. Since the expression of the EIAV vectors is driven by the cytomegalovirus promoter, this result would agree with a previous study of Zhang et al., where the authors concluded that human A3B is able to inhibit transcription of simian virus 40 and cytomegalovirus promoters (99). Again, CrFK cells were infected with vector stocks normalized for RT, and 3 days postinfection the cells were used to quantify intracellular luciferase activity. As shown in Fig. 3A and 7, human A3F and -G, muA3Z2-Z3, and porcine A3Z2-Z3 proteins were found to exert a significant inhibitory effect on the infectivity of EIAV. Specifically, human A3G and porcine A3Z2-Z3 reduced the infectivity of EIAV 90-fold and 145-fold, respectively. The other tested human and nonprimate A3s showed no effect or a very weak inhibitory effect against EIAV. Human A3s were packaged in EIAV independent of their antiviral activity, with the notable exception of human A3H (Fig. 3D).

A single amino acid mutation in the active site of eqA3Z3 results in loss of antiviral activity. Because of the difficulties in detecting eqA3-derived cytidine deamination in EIAV genomes, we studied the relevance of the zinc coordination domain for the antiviral activity. It has been reported that cytidine deamination is largely dispensable for the inhibition HIV-1 Δ*vif* by human A3F and A3G (4, 30, 46, 61). But controversially, several groups have reported a significant drop in inhibition observed when active-site mutants of human A3G were analyzed (8, 9, 22, 23, 56, 75). To address this question for EIAV, we analyzed four previously described human A3F and -G mutants called h3FAS1, h3FAS2, h3FAS1/2, and A3G-E259Q (7, 23). Additionally, we generated four eqA3Z3 mutants with related changes at the important amino acid positions of the Zn^{2+} coordinating site. Human A3F and -G contain two Zn^{2+} coordinating sites; only the CT Zn^{2+} coordinating sites are enzymatically active while the amino-terminal Zn^{2+} coordinating sites have been proposed to play a role in the specific packaging of these two A3s into HIV-1 Δ*vif* particles (23, 60). In A3G-E259Q, a glutamic acid residue at position 259 has been mutated to glutamine, which results in loss of the cytidine deaminase activity of A3G (7). The catalytic glutamic acid residues of the amino-terminal cytidine deaminase domain (CDD) in the A3F mutant h3FAS1 and of the CT CDD in h3FAS2 are changed to alanines, and h3FAS1/2 carries both point mutations (23). For eqA3Z3, in the single CDD the mutations H84R, E86Q, C115S, and C118S were gener-

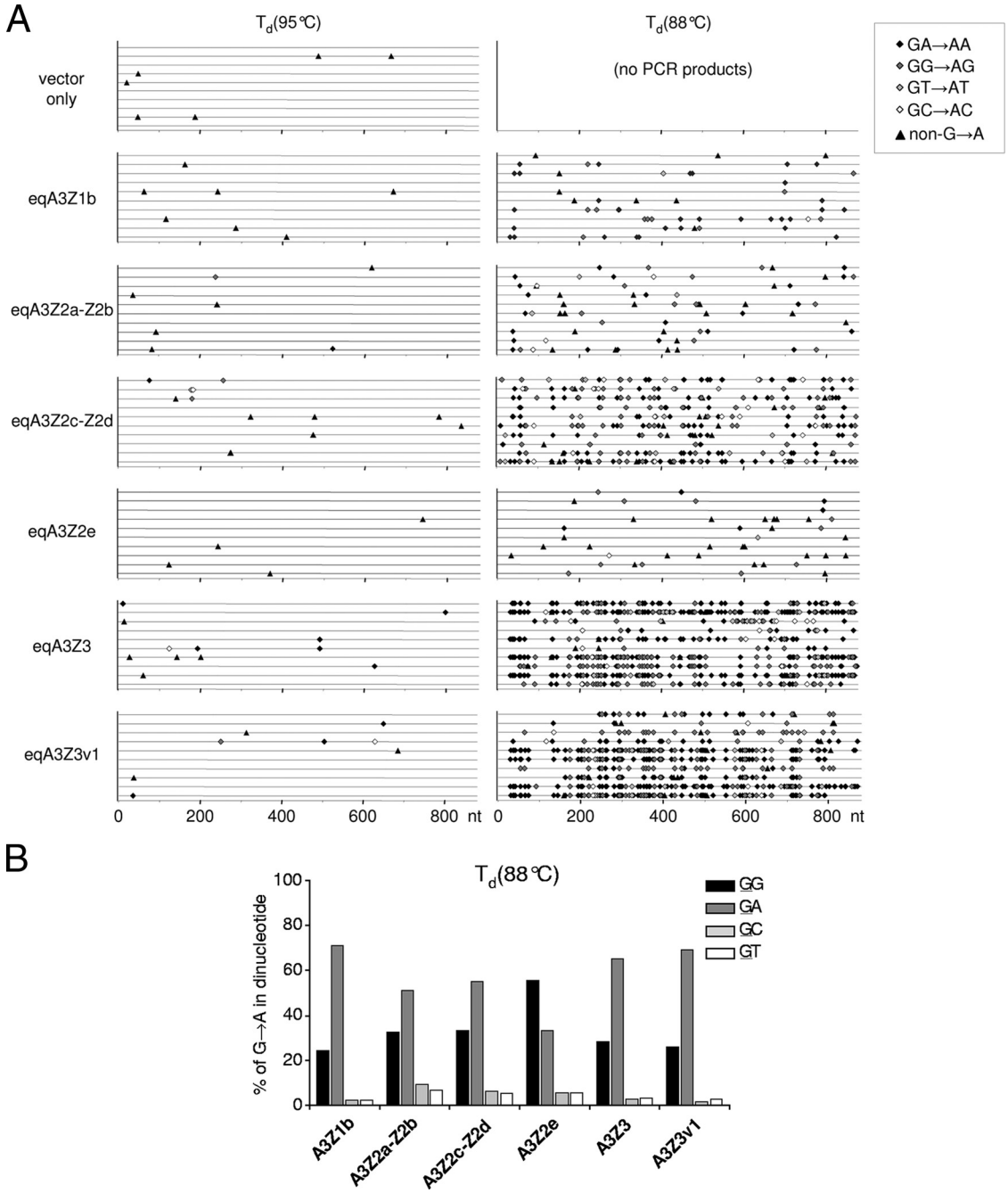

FIG. 5. eqA3 triggers G-to-A hypermutation in a subpopulation of the EIAV-luc genomes. (A) EIAV vector sequences (880 nucleotides [nt] of the luciferase gene) amplified by PCR at 10 h postinfection from CrFK cells transduced by EIAV generated in the presence or absence of eqA3Z1b, eqA3Z2a-Z2b, eqA3Z2c-Z2d, eqA3Z2e, eqA3Z3, and eqA3Z3v1. The mutations of 10 individual clones of each group are shown. Each mutation is indicated and coded with respect to the nucleotide mutation. PCR was done at a denaturation temperature (T_d) of either 95°C or of 88°C. (B) Comparison of the dinucleotide sequence context of G (underlined) →A mutations in the positive-strand DNA of EIAV-luc derived from eqA3-expressing 293T cells.

ated, resulting in eqA3Z3-H84R, -H86Q, -C115S, and -C118S, respectively. Analyses of the effect of the A3F and A3G mutants on EIAV infectivity showed that the A3 CT mutants lost all or most of the antiviral activity: h3FAS2 and hA3FAS1/2 reduced the infectivity only two- to threefold, and A3G-E259Q showed no inhibitory effect; wt A3F and the mutant h3FAS1 inhibited EIAV 10- and 15-fold, respectively (Fig. 8A). The mutant h3FAS1 was slightly more active than the wt human A3F, an effect also observed by Hakata et al. in connection with HIV-1 Δ*vif* (23). The protein A3G-E259Q showed a reduced packaging, while all other active-site mutants were found in EIAV particles at amounts similar to wt proteins (Fig. 8B). The eqA3Z3 mutants showed weak antiviral activity and inhibited EIAV only twofold (Fig. 8A). We conclude that the

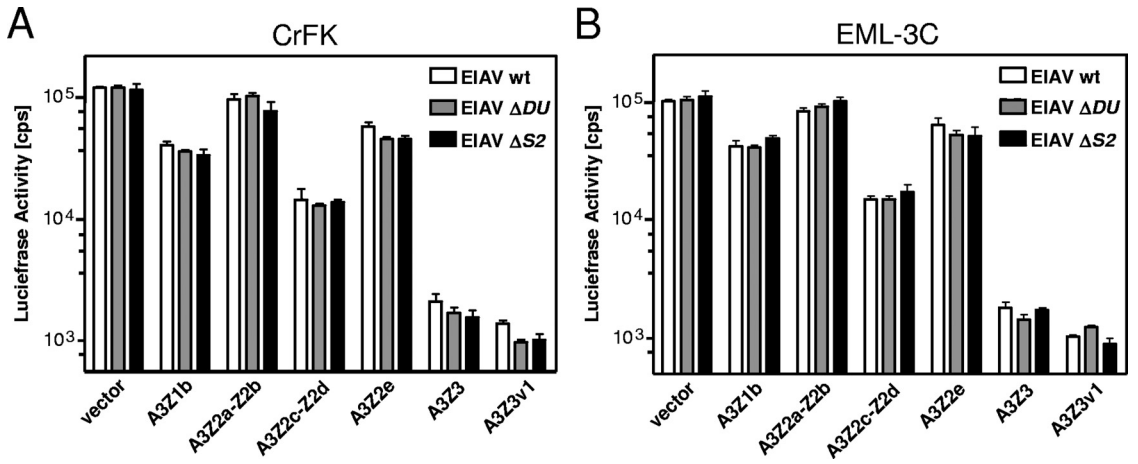

FIG. 6. Inhibition of EIAV by eqA3s is independent from dUTPase and S2. wt, ΔDU, and ΔS2 EIAV viruses were produced in the presence or absence of the indicated HA-tagged A3 expression vectors. Relative infectivity of equal amounts of the reporter viruses was determined by quantification of luciferase activity in CrFK cells (A) or EML-3C macrophage-like cells (B) at 3 days postinfection. cps, counts per second.

CT CDDs of human A3F and -G also play an essential role in the inhibition of EIAV and that the CDD of eqA3Z3 is important even though CDD mutants of eqA3Z3 remain partially active against EIAV.

DISCUSSION

The evolution of A3 genes tells us a story of gene duplication and specialization throughout mammalian history. Three main clades can be distinguished within the A3 genes, namely A3Z1, A3Z2, and A3Z3. The distribution supports the hypothesis of an ancient origin of the A3 genes in the proto-mammalian genome, followed by early duplication events before the appearance of the main clades within Mammalia (38, 58). In this sense, the chromosomal arrangement of the A3 genes in the horse genome is paradigmatic: two copies of the A3Z1 genes, followed by five copies in tandem of the A3Z2 genes, and a single copy of the A3Z3 gene. Regarding the two eqA3Z1 genes, a homologous canine A3Z1 gene exists as a single gene

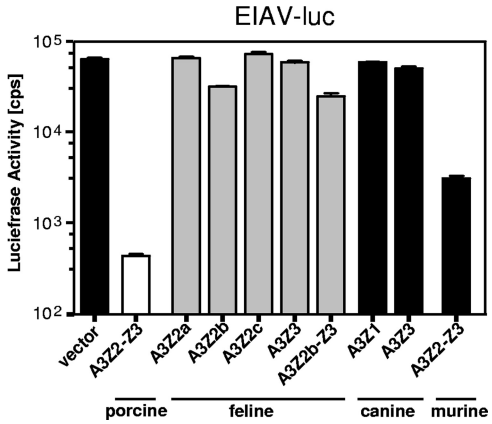

FIG. 7. Inhibition of EIAV by nonprimate A3 proteins. EIAV luciferase reporter viruses were produced in 293T cells in the presence or absence of the indicated A3s. Infectivity of the viruses was determined by quantification of luciferase activity in CrFK cells infected with equal amounts of virions at 3 days postinfection. cps, counts per second.

(58). This suggests that the extant A3Z1a and A3Z1b genes in the horse genome appeared via duplication after the last common ancestor of Carnivora and Perissodactyla, which could be dated some 62.5 million years ago (2). With respect to origins of the five eqA3Z2 genes, they all also share a common ancestor that is more recent than the last common ancestor of Perissodactyla and Carnivora and should therefore be considered inparalogs compared with the rest of the tree terminal taxa (81). In the Bayesian relaxed clock results, there are no significant differences between the heights of the nodes that define the last common ancestor of the eqA3Z1 genes (median, 0.0633; 95% confidence interval, 0.033 to 0.1034 substitutions per site) and the eqA3Z2 genes (median, 0.0742; 95% confidence interval, 0.0525 to 0.105 substitutions per site). This concordance can be interpreted to mean that both expansions, A3Z1 and A3Z2, have occurred close in time, maybe even in two simultaneous duplication events. This event(s) would have generated, on the one hand, the ancestors of the present day eqA3Z1a and eqA3Z1b and, on the other hand, the ancestor of present day eqA3Z2a-d and of eqA3Z2e (Fig. 1). After the duplication of the ancestor A3Z2a-d gene, which generated the ancestor A3Z2a,c and A3Z2b,d genes, these later genes fused and formed after an additional duplication the present A3Z2a-Z2b and A3Z2c-Z2d double-domain A3 genes. While the ancestor A3Z2a-d was involved in several genetic rearrangements, the A3Z2e gene was preserved. Further research will be necessary to determine whether the additional duplications of the A3Z1 genes and of the A3Z2 genes in horse are shared also by other species within the genus *Equus* (such as zebra or donkey) or by other genera within the order Perissodactyla (such as Rhinocerotidae or Tapiridae). Recently, read-through transcripts of A3Z2 and A3Z3 genes have been identified in cats and pigs (38, 58). We could not find such a transcript in our equine cDNA samples. But very interestingly, an equine read-through transcript is deposited in the GenBank database (RNA molecule accession number XM_001501833). This at least implies that some individual horses do express an additional A3.

Within the placentalia superorder of Laurasiatheria, A3Z2

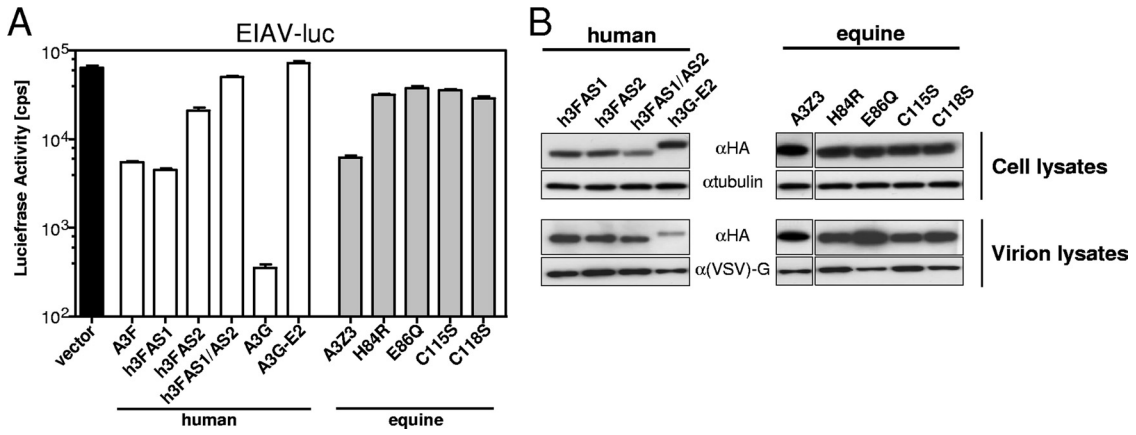

FIG. 8. Analysis of human A3F and A3G and eqA3Z3 active-site mutants for antiviral activity. (A) Different active-site mutants of human A3F and A3G and eqA3Z3 (A3Z3) were tested for antiviral activity against EIAV-luc produced in 293T cells by cotransfection with wt or mutant A3 expression plasmids. Transfection with pcDNA3.1 (vector) instead of the A3 expression plasmid was included as a control. CrFK target cells were infected with virus-containing supernatants normalized for RT, and luciferase was measured at 3 days postinfection. (B) Virions were generated by cotransfection of 293T cells with EIAV-luc and mutant HA-tagged eqA3 and human A3 expression plasmids or pcDNA3.1 (vector). A3 expression in transfected cells was detected by immunoblotting using anti-HA antibodies. Cell lysates were also analyzed for equal amounts of total proteins by using anti-tubulin antibody. Packaged A3s in virions normalized by RT activity were detected by probing with anti-HA antibody. Immunoblots of virions were also probed with anti-VSV-G antibody as a control for equal particle loading. α, anti.

genes have also undergone several duplication rounds in cats (58). Remarkably, the A3Z3 gene was never amplified and has been preserved as a single gene in Felidae and in Equidae. A similar situation is found within the superorder of Euarchontoglires in humans/primates, where after the amplification of A3Z2 and A3Z1, the duplicated genes fused and formed double-domain A3 genes (human A3B, -DE, -F, and -G) (37, 58). Amplified A3Z3 genes have not been found, and in contrast to amplification of A3Z1 and A3Z2 genes, it seems to be an evolutionary disadvantage. Consistent with this hypothesis, it was recently shown that nonfunctional human A3Z3 alleles are highly prevalent and have been actively selected for (24, 62).

The discovery of the cellular antiviral cytidine deaminase A3G in search for the Vif cofactor explained many in vitro observations regarding the replication of HIV-1 and HIV-1 Δ*vif* in specific human cells (5, 49, 78, 91, 100). It also contributed to explain the narrow host range of HIV-1 that shows spreading replication only in humans and chimpanzees (49, 59). Such defined interactions of Vif proteins with cognate A3 proteins had been shown so far only for HIV, SIV, and *Feline immunodeficiency virus* (49, 58, 74). But the discovery of the Vif-A3 interaction also highlighted the conundrum of "simple" mammalian retroviruses like Mo-MLV and *Mouse mammary tumor virus* and their survival without accessory genes like the *vif* gene (45,64–66). If simple retroviruses do get along without encoding proteins that actively counteract the impact of antiviral A3s, it is unclear why lentiviruses have evolved or retained the *vif* gene. A Vif-deficient lentivirus like EIAV might therefore be a possible evolutionary link to understand the biological relevance of Vif and to further investigate the question whether a virus is targeted by its species-own A3s (70). Equine PBMCs express at least five different types of A3 genes. EIAV was mostly sensitive to eqA3Z3 and eqA3Z2c-Z2d and was only weakly inhibited by eqA3Z1b, eqA3Z2a-Z2b, and -Z2e. However in macrophages, the natural target cells of EIAV, anti-EIAV A3s (A3Z2c-Z2d and A3Z3) are expressed at low levels or barely expressed. Some reports have suggested a requirement for the S2 gene for high virus loads in vivo and disease induction (19, 42). Our finding that EIAV S2 does not affect susceptibility to eqA3s is consistent with studies by Li et al. (43), who have recently shown that S2 is not required for viral replication in vitro in several equine cell lines and macrophages. In contrast, the dUTPase of EIAV is necessary for viral replication in macrophages (17). Our data clearly show that EIAV dUTPase does not protect against eqA3s. How does EIAV survive and replicate without any A3-counteracting viral function? We propose that EIAV may use multiple strategies to interact with its species-own A3s: it tolerates packaging of eqA3s that are not active against EIAV (A3Z1b, A3Z2a-Z2b, and A3Z2e) and avoids the active antiviral eqA3Z3 by an evolutionary adaption of its cellular tropism to macrophages that showed very low expression levels of A3Z3. The A3Z2c-Z2d was also active against EIAV and found to be expressed at low levels in macrophages. Interestingly, the sequence of the eqA3Z2c-Z2d of our horse samples compared with the sequences of Bogerd et al. (6) differed in four amino acids. This genetic variation in A3Z2c-Z2ds influenced its anti-EIAV activity significantly (Fig. 4A). Future experimental investigations and field studies are required to support our hypothesis that the presence of these or other A3 single nucleotide polymorphisms and the expression of A3Z2-Z3 read-through transcripts modulate the susceptibility of horses to EIAV infection and disease induction.

The evolutionary history of the A3 genes shows a clear tendency toward the growth of the antiviral protein armory. This increase proceeds through gene duplication and possibly also gene fusion and alternative read-through mechanisms. Since gene fusion is more common than gene fission (36), it is tempting to speculate that the read-through mechanism could act as a preadaptation, facilitating—even mechanistically—the gene fusion event. The diversification of genes opens the door to neofunctionalization (29) and/or subfunctionalization (47). Under

the "duplication-degeneration-complementation" model, mechanisms that tend to preserve the duplicated genes act by partitioning the original functions in the ancestral gene between the sister genes rather than generating new functions (21). We have shown here that present-day eqA3 proteins appeared after recent gene duplication events, have different cellular localizations, and display different activities against distinct viruses, and this is also true for other species (58). In this sense, the different eqA3Z1 and eqA3Z2 proteins, the different human A3Z2-Z2 and -Z2-Z1 proteins, the different feline A3Z2 proteins, and even A3Z2-Z3 readthrough transcription products (38, 58) might be regarded as specialized antiviral proteins that have evolved, taking over and refining ancestral functions in the original gene. Alternatively, if the evolutionary forces that have independently favored the conservation of the duplicated A3 genes in Equidae, in Felidae, and in primates parallel the pressure that retroviruses pose on their hosts, the maintenance of the duplicated genes in the host genome might reflect an increase in the retroviral diversity affecting specific taxa at specific time points.

ACKNOWLEDGMENTS

We thank Cheik Coulibali, Roland Plesker, Thomas Sternsdorf, Juri Vogel, Carina Meyer, and Sabrina Janßen for expert technical assistance and Eva Dörrschuck, Susan Kingsman, Nathanial R. Landau, Kyri Mitrophanous, Ronald C. Montelaro, Gerhard Pietsch, Barbara Schnierle, Ralf Tönjes, and Yong-Hui Zheng for the gift of reagents. We thank Hartmut Hengel and Dieter Häussinger for support.

IGB is funded by the Volkswagen Foundation and by the Programa Ramón y Cajal, Ministry of Science and Innovation, Spain. The project was funded in part by DFG grant MU 1608/4-1 to C.M. C.M. is supported by the Heinz-Ansmann Foundation for AIDS Research.

REFERENCES

1. **Balaggan, K. S., K. Binley, M. Esapa, S. Iqball, Z. Askham, O. Kan, M. Tschernutter, J. W. Bainbridge, S. Naylor, and R. R. Ali.** 2006. Stable and efficient intraocular gene transfer using pseudotyped EIAV lentiviral vectors. J. Gene Med. **8:**275–285.
2. **Benton, M. J., and P. C. Donoghue.** 2007. Paleontological evidence to date the tree of life. Mol. Biol. Evol. **24:**26–53.
3. **Bininda-Emonds, O. R., M. Cardillo, K. E. Jones, R. D. MacPhee, R. M. Beck, R. Grenyer, S. A. Price, R. A. Vos, J. L. Gittleman, and A. Purvis.** 2007. The delayed rise of present-day mammals. Nature **446:**507–512.
4. **Bishop, K. N., R. K. Holmes, and M. H. Malim.** 2006. Antiviral potency of APOBEC proteins does not correlate with cytidine deamination. J. Virol. **80:**8450–8458.
5. **Bishop, K. N., R. K. Holmes, A. M. Sheehy, N. O. Davidson, S. J. Cho, and M. H. Malim.** 2004. Cytidine deamination of retroviral DNA by diverse APOBEC proteins. Curr. Biol. **14:**1392–1396.
6. **Bogerd, H. P., R. L. Tallmadge, J. L. Oaks, S. Carpenter, and B. R. Cullen.** 2008. Equine infectious anemia virus resists the antiretroviral activity of equine APOBEC3 proteins through a packaging-independent mechanism. J. Virol. **82:**11889–11901.
7. **Bogerd, H. P., H. L. Wiegand, B. P. Doehle, and B. R. Cullen.** 2007. The intrinsic antiretroviral factor APOBEC3B contains two enzymatically active cytidine deaminase domains. Virology **364:**486–493.
8. **Browne, E. P., C. Allers, and N. R. Landau.** 2009. Restriction of HIV-1 by APOBEC3G is cytidine deaminase-dependent 1. Virology **387:**313–321.
9. **Browne, E. P., and D. R. Littman.** 2008. Species-specific restriction of APOBEC3-mediated hypermutation. J. Virol. **82:**1305–1313.
10. **Craigo, J. K., S. Durkin, T. J. Sturgeon, T. Tagmyer, S. J. Cook, C. J. Issel, and R. C. Montelaro.** 2007. Immune suppression of challenged vaccinates as a rigorous assessment of sterile protection by lentiviral vaccines. Vaccine **25:**834–845.
11. **Dang, Y., X. Wang, W. J. Esselman, and Y. H. Zheng.** 2006. Identification of APOBEC3DE as another antiretroviral factor from the human APOBEC family. J. Virol. **80:**10522–10533.
12. **Derse, D., S. A. Hill, G. Princler, P. Lloyd, and G. Heidecker.** 2007. Resistance of human T cell leukemia virus type 1 to APOBEC3G restriction is mediated by elements in nucleocapsid. Proc. Natl. Acad. Sci. USA **104:**2915–2920.
13. **Doehle, B. P., A. Schafer, H. L. Wiegand, H. P. Bogerd, and B. R. Cullen.** 2005. Differential sensitivity of murine leukemia virus to APOBEC3-mediated inhibition is governed by virion exclusion. J. Virol. **79:**8201–8207.
14. **Drummond, A. J., and A. Rambaut.** 2007. BEAST: Bayesian evolutionary analysis by sampling trees. BMC Evol. Biol. **7:**214.
15. **Edgar, R. C.** 2004. MUSCLE: a multiple sequence alignment method with reduced time and space complexity. BMC Bioinformatics **5:**113.
16. **Edgar, R. C.** 2004. MUSCLE: multiple sequence alignment with high accuracy and high throughput. Nucleic Acids Res. **32:**1792–1797.
17. **Elder, J. H., D. L. Lerner, C. S. Hasselkus-Light, D. J. Fontenot, E. Hunter, P. A. Luciw, R. C. Montelaro, and T. R. Phillips.** 1992. Distinct subsets of retroviruses encode dUTPase 3. J. Virol. **66:**1791–1794.
18. **Emi, N., T. Friedmann, and J. K. Yee.** 1991. Pseudotype formation of murine leukemia virus with the G protein of vesicular stomatitis virus. J. Virol. **65:**1202–1207.
19. **Fagerness, A. J., M. T. Flaherty, S. T. Perry, B. Jia, S. L. Payne, and F. J. Fuller.** 2006. The S2 accessory gene of equine infectious anemia virus is essential for expression of disease in ponies 1. Virology **349:**22–30.
20. **Fidalgo-Carvalho, I., J. K. Craigo, S. Barnes, C. Costa-Ramos, and R. C. Montelaro.** 2009. Characterization of an equine macrophage cell line: application to studies of EIAV infection 1. Vet. Microbiol. **136:**8–19.
21. **Force, A., M. Lynch, F. B. Pickett, A. Amores, Y. L. Yan, and J. Postlethwait.** 1999. Preservation of duplicate genes by complementary, degenerative mutations. Genetics **151:**1531–1545.
22. **Hache, G., M. T. Liddament, and R. S. Harris.** 2005. The retroviral hypermutation specificity of APOBEC3F and APOBEC3G is governed by the C-terminal DNA cytosine deaminase domain. J. Biol. Chem. **280:**10920–10924.
23. **Hakata, Y., and N. R. Landau.** 2006. Reversed functional organization of mouse and human APOBEC3 cytidine deaminase domains. J. Biol. Chem. **281:**36624–36631.
24. **Harari, A., M. Ooms, L. C. Mulder, and V. Simon.** 2009. Polymorphisms and splice variants influence the antiretroviral activity of human APOBEC3H. J. Virol. **83:**295–303.
25. **Harris, R. S., K. N. Bishop, A. M. Sheehy, H. M. Craig, S. K. Petersen-Mahrt, I. N. Watt, M. S. Neuberger, and M. H. Malim.** 2003. DNA deamination mediates innate immunity to retroviral infection. Cell **113:**803–809.
26. **Hatziioannou, T., D. Perez-Caballero, A. Yang, S. Cowan, and P. D. Bieniasz.** 2004. Retrovirus resistance factors Ref1 and Lv1 are species-specific variants of TRIM5α. Proc. Natl. Acad. Sci. USA **101:**10774–10779.
27. **Holmes, R. K., F. A. Koning, K. N. Bishop, and M. H. Malim.** 2007. APOBEC3F can inhibit the accumulation of HIV-1 reverse transcription products in the absence of hypermutation. Comparisons with APOBEC3G. J. Biol. Chem. **282:**2587–2595.
28. **Holmes, R. K., M. H. Malim, and K. N. Bishop.** 2007. APOBEC-mediated viral restriction: not simply editing? Trends Biochem. Sci. **32:**118–128.
29. **Hughes, T., and D. A. Liberles.** 2007. The pattern of evolution of smaller-scale gene duplicates in mammalian genomes is more consistent with neo-than subfunctionalisation. J. Mol. Evol. **65:**574–588.
30. **Iwatani, Y., D. S. Chan, F. Wang, K. S. Maynard, W. Sugiura, A. M. Gronenborn, I. Rouzina, M. C. Williams, K. Musier-Forsyth, and J. G. Levin.** 2007. Deaminase-independent inhibition of HIV-1 reverse transcription by APOBEC3G. Nucleic Acids Res. **35:**7096–7108.
31. **Jarmuz, A., A. Chester, J. Bayliss, J. Gisbourne, I. Dunham, J. Scott, and N. Navaratnam.** 2002. An anthropoid-specific locus of orphan C to U RNA-editing enzymes on chromosome 22. Genomics **79:**285–296.
32. **Jern, P., J. P. Stoye, and J. M. Coffin.** 2007. Role of APOBEC3 in genetic diversity among endogenous murine leukemia viruses. PLoS Genet. **3:**2014–2022.
33. **Jonsson, S. R., G. Hache, M. D. Stenglein, S. C. Fahrenkrug, V. Andresdottir, and R. S. Harris.** 2006. Evolutionarily conserved and non-conserved retrovirus restriction activities of artiodactyl APOBEC3F proteins. Nucleic Acids Res. **34:**5683–5694.
34. **Katzourakis, A., M. Tristem, O. G. Pybus, and R. J. Gifford.** 2007. Discovery and analysis of the first endogenous lentivirus. Proc. Natl. Acad. Sci. USA **104:**6261–6265.
35. **Kobayashi, M., A. Takaori-Kondo, K. Shindo, A. Abudu, K. Fukunaga, and T. Uchiyama.** 2004. APOBEC3G targets specific virus species. J. Virol. **78:**8238–8244.
36. **Kummerfeld, S. K., and S. A. Teichmann.** 2005. Relative rates of gene fusion and fission in multi-domain proteins. Trends Genet. **21:**25–30.
37. **LaRue, R. S., V. Andresdottir, Y. Blanchard, S. G. Conticello, D. Derse, M. Emerman, W. C. Greene, S. R. Jonsson, N. R. Landau, M. Löchelt, H. S. Malik, M. H. Malim, C. Münk, S. J. O'Brien, V. K. Pathak, K. Strebel, S. Wain-Hobson, X. F. Yu, N. Yuhki, and R. S. Harris.** 2009. Guidelines for naming nonprimate APOBEC3 genes and proteins. J. Virol. **83:**494–497.
38. **LaRue, R. S., S. R. Jonsson, K. A. Silverstein, M. Lajoie, D. Bertrand, N. El-Mabrouk, I. Hotzel, V. Andresdottir, T. P. Smith, and R. S. Harris.** 2008. The artiodactyl APOBEC3 innate immune repertoire shows evidence for a multi-functional domain organization that existed in the ancestor of placental mammals. BMC Mol. Biol. **9:**104.
39. **Lecossier, D., F. Bouchonnet, F. Clavel, and A. J. Hance.** 2003. Hypermutation of HIV-1 DNA in the absence of the Vif protein. Science **300:**1112.
40. **Leroux, C., J. L. Cadore, and R. C. Montelaro.** 2004. Equine Infectious

Anemia Virus (EIAV): what has HIV's country cousin got to tell us? Vet. Res. **35:**485–512.
41. **Leroux, C., J. K. Craigo, C. J. Issel, and R. C. Montelaro.** 2001. Equine infectious anemia virus genomic evolution in progressor and nonprogressor ponies. J. Virol. **75:**4570–4583.
42. **Li, F., C. Leroux, J. K. Craigo, S. J. Cook, C. J. Issel, and R. C. Montelaro.** 2000. The S2 gene of equine infectious anemia virus is a highly conserved determinant of viral replication and virulence properties in experimentally infected ponies. J. Virol. **74:**573–579.
43. **Li, F., B. A. Puffer, and R. C. Montelaro.** 1998. The S2 gene of equine infectious anemia virus is dispensable for viral replication in vitro. J. Virol. **72:**8344–8348.
44. **Löchelt, M., F. Romen, P. Bastone, H. Muckenfuss, N. Kirchner, Y. B. Kim, U. Truyen, U. Rosler, M. Battenberg, A. Saib, E. Flory, K. Cichutek, and C. Münk.** 2005. The antiretroviral activity of APOBEC3 is inhibited by the foamy virus accessory Bet protein. Proc. Natl. Acad. Sci. USA **102:**7982–7987.
45. **Low, A., C. M. Okeoma, N. Lovsin, H. M. de las, T. H. Taylor, B. M. Peterlin, S. R. Ross, and H. Fan.** 2009. Enhanced replication and pathogenesis of Moloney murine leukemia virus in mice defective in the murine APOBEC3 gene. Virology **385:**455–463.
46. **Luo, K., T. Wang, B. Liu, C. Tian, Z. Xiao, J. Kappes, and X. F. Yu.** 2007. Cytidine deaminases APOBEC3G and APOBEC3F interact with human immunodeficiency virus type 1 integrase and inhibit proviral DNA formation. J. Virol. **81:**7238–7248.
47. **Lynch, M., and A. Force.** 2000. The probability of duplicate gene preservation by subfunctionalization. Genetics **154:**459–473.
48. **Mangeat, B., P. Turelli, G. Caron, M. Friedli, L. Perrin, and D. Trono.** 2003. Broad antiretroviral defence by human APOBEC3G through lethal editing of nascent reverse transcripts. Nature **424:**99–103.
49. **Mariani, R., D. Chen, B. Schröfelbauer, F. Navarro, R. König, B. Bollman, C. Münk, H. Nymark-McMahon, and N. R. Landau.** 2003. Species-specific exclusion of APOBEC3G from HIV-1 virions by Vif. Cell **114:**21–31.
50. **Marin, M., K. M. Rose, S. L. Kozak, and D. Kabat.** 2003. HIV-1 Vif protein binds the editing enzyme APOBEC3G and induces its degradation. Nat. Med. **9:**1398–1403.
51. **Matsushita, T., S. Elliger, C. Elliger, G. Podsakoff, L. Villarreal, G. J. Kurtzman, Y. Iwaki, and P. Colosi.** 1998. Adeno-associated virus vectors can be efficiently produced without helper virus. Gene Ther. **5:**938–945.
52. **Maury, W.** 1994. Monocyte maturation controls expression of equine infectious anemia virus. J. Virol. **68:**6270–6279.
53. **Mazarakis, N. D., M. Azzouz, J. B. Rohll, F. M. Ellard, F. J. Wilkes, A. L. Olsen, E. E. Carter, R. D. Barber, D. F. Baban, S. M. Kingsman, A. J. Kingsman, K. O'Malley, and K. A. Mitrophanous.** 2001. Rabies virus glycoprotein pseudotyping of lentiviral vectors enables retrograde axonal transport and access to the nervous system after peripheral delivery. Hum. Mol. Genet. **10:**2109–2121.
54. **Mbisa, J. L., R. Barr, J. A. Thomas, N. Vandegraaff, I. J. Dorweiler, E. S. Svarovskaia, W. L. Brown, L. M. Mansky, R. J. Gorelick, R. S. Harris, A. Engelman, and V. K. Pathak.** 2007. Human immunodeficiency virus type 1 cDNAs produced in the presence of APOBEC3G exhibit defects in plus-strand DNA transfer and integration. J. Virol. **81:**7099–7110.
55. **Mitrophanous, K., S. Yoon, J. Rohll, D. Patil, F. Wilkes, V. Kim, S. Kingsman, A. Kingsman, and N. Mazarakis.** 1999. Stable gene transfer to the nervous system using a non-primate lentiviral vector. Gene Ther. **6:**1808–1818.
56. **Miyagi, E., S. Opi, H. Takeuchi, M. Khan, R. Goila-Gaur, S. Kao, and K. Strebel.** 2007. Enzymatically active APOBEC3G is required for efficient inhibition of human immunodeficiency virus type 1. J. Virol. **81:**13346–13353.
57. **Muckenfuss, H., M. Hamdorf, U. Held, M. Perkovic, J. Löwer, K. Cichutek, E. Flory, G. G. Schumann, and C. Münk.** 2006. APOBEC3 proteins inhibit human LINE-1 retrotransposition. J. Biol. Chem. **281:**22161–22172.
58. **Münk, C., T. Beck, J. Zielonka, A. Hotz-Wagenblatt, S. Chareza, M. Battenberg, J. Thielebein, K. Cichutek, I. G. Bravo, S. J. O'Brien, M. Löchelt, and N. Yuhki.** 2008. Functions, structure, and read-through alternative splicing of feline APOBEC3 genes. Genome Biol. **9:**R48.
59. **Münk, C., J. Zielonka, H. Constabel, B. P. Kloke, B. Rengstl, M. Battenberg, F. Bonci, M. Pistello, M. Löchelt, and K. Cichutek.** 2007. Multiple restrictions of human immunodeficiency virus type 1 in feline cells. J. Virol. **81:**7048–7060.
60. **Navarro, F., B. Bollman, H. Chen, R. König, Q. Yu, K. Chiles, and N. R. Landau.** 2005. Complementary function of the two catalytic domains of APOBEC3G. Virology **333:**374–386.
61. **Newman, E. N., R. K. Holmes, H. M. Craig, K. C. Klein, J. R. Lingappa, M. H. Malim, and A. M. Sheehy.** 2005. Antiviral function of APOBEC3G can be dissociated from cytidine deaminase activity. Curr. Biol. **15:**166–170.
62. **OhAinle, M., J. A. Kerns, M. M. Li, H. S. Malik, and M. Emerman.** 2008. Antiretroelement activity of APOBEC3H was lost twice in recent human evolution. Cell Host Microbe **4:**249–259.
63. **OhAinle, M., J. A. Kerns, H. S. Malik, and M. Emerman.** 2006. Adaptive evolution and antiviral activity of the conserved mammalian cytidine deaminase APOBEC3H. J. Virol. **80:**3852–3862.
64. **Okeoma, C. M., N. Lovsin, B. M. Peterlin, and S. R. Ross.** 2007. APOBEC3 inhibits mouse mammary tumour virus replication in vivo. Nature **445:**927–930.
65. **Okeoma, C. M., A. Low, W. Bailis, H. Y. Fan, B. M. Peterlin, and S. R. Ross.** 2009. Induction of APOBEC3 in vivo causes increased restriction of retrovirus infection. J. Virol. **83:**3486–3495.
66. **Okeoma, C. M., J. Petersen, and S. R. Ross.** 2009. Expression of murine APOBEC3 alleles in different mouse strains and their effect on mouse mammary tumor virus infection. J. Virol. **83:**3029–3038.
67. **O'Rourke, J. P., H. Hiraragi, K. Urban, M. Patel, J. C. Olsen, and B. A. Bunnell.** 2003. Analysis of gene transfer and expression in skeletal muscle using enhanced EIAV lentivirus vectors. Mol. Ther. **7:**632–639.
68. **Radcliffe, P. A., C. J. Sion, F. J. Wilkes, E. J. Custard, G. L. Beard, S. M. Kingsman, and K. A. Mitrophanous.** 2008. Analysis of factor VIII mediated suppression of lentiviral vector titres. Gene Ther. **15:**289–297.
69. **Rohll, J. B., K. A. Mitrophanous, E. Martin-Rendon, F. M. Ellard, P. A. Radcliffe, N. D. Mazarakis, and S. M. Kingsman.** 2002. Design, production, safety, evaluation, and clinical applications of nonprimate lentiviral vectors. Methods Enzymol. **346:**466–500.
70. **Ross, S. R.** 2009. Are viruses inhibited by APOBEC3 molecules from their host species? PLoS Pathog **5:**e1000347.
71. **Russell, R. A., H. L. Wiegand, M. D. Moore, A. Schafer, M. O. McClure, and B. R. Cullen.** 2005. Foamy virus Bet proteins function as novel inhibitors of the APOBEC3 family of innate antiretroviral defense factors. J. Virol. **79:**8724–8731.
72. **Saenz, D. T., W. Teo, J. C. Olsen, and E. M. Poeschla.** 2005. Restriction of feline immunodeficiency virus by Ref1, Lv1, and primate TRIM5α proteins. J. Virol. **79:**15175–15188.
73. **Santiago, M. L., M. Montano, R. Benitez, R. J. Messer, W. Yonemoto, B. Chesebro, K. J. Hasenkrug, and W. C. Greene.** 2008. Apobec3 encodes Rfv3, a gene influencing neutralizing antibody control of retrovirus infection. Science **321:**1343–1346.
74. **Schröfelbauer, B., D. Chen, and N. R. Landau.** 2004. A single amino acid of APOBEC3G controls its species-specific interaction with virion infectivity factor (Vif). Proc. Natl. Acad. Sci. USA **101:**3927–3932.
75. **Schumacher, A. J., G. Hache, D. A. Macduff, W. L. Brown, and R. S. Harris.** 2008. The DNA deaminase activity of human APOBEC3G is required for Ty1, MusD, and human immunodeficiency virus type 1 restriction. J. Virol. **82:**2652–2660.
76. **Sellon, D. C., F. J. Fuller, and T. C. McGuire.** 1994. The immunopathogenesis of equine infectious anemia virus. Virus Res. **32:**111–138.
77. **Sellon, D. C., S. T. Perry, L. Coggins, and F. J. Fuller.** 1992. Wild-type equine infectious anemia virus replicates in vivo predominantly in tissue macrophages, not in peripheral blood monocytes. J. Virol. **66:**5906–5913.
78. **Sheehy, A. M., N. C. Gaddis, J. D. Choi, and M. H. Malim.** 2002. Isolation of a human gene that inhibits HIV-1 infection and is suppressed by the viral Vif protein. Nature **418:**646–650.
79. **Sheehy, A. M., N. C. Gaddis, and M. H. Malim.** 2003. The antiretroviral enzyme APOBEC3G is degraded by the proteasome in response to HIV-1 Vif. Nat. Med. **9:**1404–1407.
80. **Shimodaira, H., and M. Hasegawa.** 1999. Multiple comparisons of log-likelihoods with applications to phylogenetic inference. Mol. Biol. Evol. **16:**1114–1116.
81. **Sonnhammer, E. L., and E. V. Koonin.** 2002. Orthology, paralogy and proposed classification for paralog subtypes. Trends Genet. **18:**619–620.
82. **Sponseller, B. A., W. O. Sparks, Y. Wannemuehler, Y. Li, A. K. Antons, J. L. Oaks, and S. Carpenter.** 2007. Immune selection of equine infectious anemia virus env variants during the long-term inapparent stage of disease. Virology **363:**156–165.
83. **Stamatakis, A.** 2006. Phylogenetic models of rate heterogeneity: a high performance computing perspective, p. 278. *In* Proceedings of the 20th IEEE International Parallel and Distributed Processing Symposium, Rhodes, Greece. IEEE Computer Society, Washington, DC. http://www2.computer.org/portal/web/csdl.
84. **Stamatakis, A.** 2006. RAxML-VI-HPC: maximum likelihood-based phylogenetic analyses with thousands of taxa and mixed models. Bioinformatics **22:**2688–2690.
85. **Stamatakis, A., T. Ludwig, and H. Meier.** 2005. RAxML-III: a fast program for maximum likelihood-based inference of large phylogenetic trees. Bioinformatics **21:**456–463.
86. **Suchard, M. A., R. E. Weiss, and J. S. Sinsheimer.** 2001. Bayesian selection of continuous-time Markov chain evolutionary models. Mol. Biol. Evol. **18:**1001–1013.
87. **Suspene, R., M. Henry, S. Guillot, S. Wain-Hobson, and J. P. Vartanian.** 2005. Recovery of APOBEC3-edited human immunodeficiency virus G→A hypermutants by differential DNA denaturation PCR. J. Gen. Virol. **86:**125–129.
88. **Suyama, M., D. Torrents, and P. Bork.** 2006. PAL2NAL: robust conversion of protein sequence alignments into the corresponding codon alignments. Nucleic Acids Res. **34:**609–612.

89. **Takeda, E., S. Tsuji-Kawahara, M. Sakamoto, M. A. Langlois, M. S. Neuberger, C. Rada, and M. Miyazawa.** 2008. Mouse APOBEC3 restricts Friend leukemia virus infection and pathogenesis in vivo. J. Virol. **82:** 10998–11008.
90. **Threadgill, D. S., W. K. Steagall, M. T. Flaherty, F. J. Fuller, S. T. Perry, K. E. Rushlow, S. F. Le Grice, and S. L. Payne.** 1993. Characterization of equine infectious anemia virus dUTPase: growth properties of a dUTPase-deficient mutant. J. Virol. **67:**2592–2600.
91. **Wiegand, H. L., B. P. Doehle, H. P. Bogerd, and B. R. Cullen.** 2004. A second human antiretroviral factor, APOBEC3F, is suppressed by the HIV-1 and HIV-2 Vif proteins. EMBO J. **23:**2451–2458.
92. **Wolf, D., and S. P. Goff.** 2008. Host restriction factors blocking retroviral replication. Annu. Rev. Genet. **42:**143–163.
93. **Xiao, X., J. Li, and R. J. Samulski.** 1998. Production of high-titer recombinant adeno-associated virus vectors in the absence of helper adenovirus. J. Virol. **72:**2224–2232.
94. **Yu, X., Y. Yu, B. Liu, K. Luo, W. Kong, P. Mao, and X. F. Yu.** 2003. Induction of APOBEC3G ubiquitination and degradation by an HIV-1 Vif-Cul5-SCF complex. Science **302:**1056–1060.
95. **Yu, Y., Z. Xiao, E. S. Ehrlich, X. Yu, and X. F. Yu.** 2004. Selective assembly of HIV-1 Vif-Cul5-ElonginB-ElonginC E3 ubiquitin ligase complex through a novel SOCS box and upstream cysteines. Genes Dev. **18:**2867–2872.
96. **Zhang, B., S. Jin, J. Jin, F. Li, and R. C. Montelaro.** 2005. A tumor necrosis factor receptor family protein serves as a cellular receptor for the macrophage-tropic equine lentivirus. Proc. Natl. Acad. Sci. USA **102:**9918–9923.
97. **Zhang, F., T. Hatziioannou, D. Perez-Caballero, D. Derse, and P. D. Bieniasz.** 2006. Antiretroviral potential of human tripartite motif-5 and related proteins. Virology **353:**396–409.
98. **Zhang, H., B. Yang, R. J. Pomerantz, C. Zhang, S. C. Arunachalam, and L. Gao.** 2003. The cytidine deaminase CEM15 induces hypermutation in newly synthesized HIV-1 DNA. Nature **424:**94–98.
99. **Zhang, W., X. Zhang, C. Tian, T. Wang, P. T. Sarkis, Y. Fang, S. Zheng, X. F. Yu, and R. Xu.** 2008. Cytidine deaminase APOBEC3B interacts with heterogeneous nuclear ribonucleoprotein K and suppresses hepatitis B virus expression. Cell Microbiol. **10:**112–121.
100. **Zheng, Y. H., D. Irwin, T. Kurosu, K. Tokunaga, T. Sata, and B. M. Peterlin.** 2004. Human APOBEC3F is another host factor that blocks human immunodeficiency virus type 1 replication. J. Virol. **78:**6073–6076.